Laser-Induced Thermal Coagulation Enhances Skin Uptake of Topically Applied Compounds

C.S. Haak, MD, PhD,[1*] J. Hannibal, MD, DMSc, PhD,[2] U. Paasch, MD, PhD,[3] R.R. Anderson, MD,[4] and M. Haedersdal, MD, DMSc, PhD[1,4]

[1]*Department of Dermatology, Bispebjerg Hospital, University of Copenhagen, Copenhagen, Denmark*
[2]*Department of Clinical Biochemistry, Bispebjerg Hospital, University of Copenhagen, Copenhagen, Denmark*
[3]*Department of Dermatology, Venereology and Allergology, University of Leipzig, Germany*
[4]*WellmanCenter for Photomedicine, Massachusetts General Hospital, Harvard Medical School, Boston, Massachusetts*

Background: Ablative fractional laser (AFL) generates microchannels in skin surrounded by a zone of thermally altered tissue, termed the coagulation zone (CZ). The thickness of CZ varies according to applied wavelength and laser settings. It is well-known that AFL channels facilitate uptake of topically applied compounds, but the importance of CZ is unknown.

Methods: Franz Cells were used to investigate skin uptake and permeation of fluorescent labeled polyethylene glycols (PEGs) with mean molecular weights (MW) of 350, 1,000, and 5,000 Da. Microchannels with CZ thicknesses ranging from 0 to 80 μm were generated from micro-needles (0 μm, CZ-0), and AFL (10,600 nm) applied to −80°C deep frozen skin (20 μm, CZ-20) and skin equilibrated to room temperature (80 μm, CZ-80). Channels penetrated into similar mid-dermal skin depths of 600–700 μm, and number of channels per skin area was similar. At 4 hours incubation, skin uptake of PEGs into CZ and dermis was evaluated by fluorescence microscopy at specific skin depths of 150, 400, and 1,000 μm and the transcutaneous permeation was quantified by fluorescence of receptor fluids.

Results: Overall, the highest uptake of PEGs was reached through microchannels surrounded by CZ compared to channels with no CZ (CZ-20 and CZ-80>CZ-0).The thickness of CZ affected PEG distribution in skin. A thin CZ-20 favored significantly higher mean fluorescence intensities inside CZ areas compared to CZ-80 (PEG 350, 1,000, and 5,000; $P < 0.001$). In dermis, the uptake through CZ-20 channels was significantly higher than through CZ-80 and CZ-0 at all skin depths (PEG 350, 1,000 and 5,000, 150–1,000 μm; $P < 0.001$). Correspondingly, transcutaneous permeation of PEG 350 was highest in CZ-20 compared to CZ-80 and CZ-0 samples ($P < 0.001$). Permeation of larger molecules (PEG 1,000 and PEG 5,000) was generally low.

Conclusion: Uptake of topical compounds is higher through microchannels surrounded by a CZ than without a CZ. Moreover, CZ thickness influences PEG distribution, with highest PEG uptake achieved from microchannels surrounded by a thin CZ. Lasers Surg. Med. 49:582–591, 2017. © 2017 Wiley Periodicals, Inc.

Key words: ablative fractional laser; coagulation zone; Franz cell; topical drug delivery

INTRODUCTION

The concept of fractional photothermolysis was first described in 2004. Initial studies used non-ablative 1, 5 μm wavelength laser beams to generate microscopic thermal skin injuries with intervening intact skin areas [1]. Later the technique was advanced to include devices operating at far infrared ablative wavelengths and thus, the ablative fractional laser (AFL) was introduced in 2007 [2,3].

Available AFLs operate at wavelengths of 2,790 nm (yttrium scandium gallium garnet, YSGG), 2,940 nm (erbium: yttrium aluminium garnet, Er:YAG) and 10,600 nm (carbon dioxide, CO_2), all wavelengths strongly absorbed by water. Accordingly, AFL exposure vaporizes microchannels in the skin and due to collateral deposition of heat into surrounding skin, the ablated channels are enclosed by a zone of thermally damaged tissue. The zone of thermally damaged tissue is referred to as the coagulation zone (CZ) and all together the ablated microchannel with surrounding CZ constitutes a microscopic treatment zone (MTZ) [4–7].

The thickness of the CZ surrounding each microchannel is variable and dependent upon laser wavelength, beam diameter, pulse duration, and pulse energy. Regarding laser wavelength, the absorption coefficient of water is an order of magnitude greater at 2,940 nm (Er:YAG) than at 10,600 nm (CO_2). Consequently, Er:YAG lasers hold the potential to generate MTZ with a thin CZ typically around 20 μm whereas CO_2 lasers generate a higher degree of

Conflict of Interest Disclosures: All authors have completed and submitted the ICMJE Form for Disclosure of Potential Conflicts of Interest and none were reported.

Contract grant sponsor: Novo Nordisk Foundation; Contract grant number: NNF—13OC0007917; Contract grant sponsor: Bispebjerg Hospital's Foundation for Health Research.

*Correspondence to: Christina Skovbølling Haak, MD, PhD, Department of Dermatology D-92, Bispebjerg Hospital, University of Copenhagen, Bispebjerg Bakke 23, DK-2400 Copenhagen NV, Denmark. E-mail: christinahaak@dadlnet.dk

Accepted 14 January 2017
Published online 9 February 2017 in Wiley Online Library (wileyonlinelibrary.com).
DOI 10.1002/lsm.22642

thermal damage in surrounding tissue, with CZ typically ranging from 60 to 90 μm [7–10]. The thickness of the CZ is also highly influenced by specific laser settings. With longer pulse durations and use of pulse stacking the CZ thickness increases due to heat accumulation in skin structures. Therefore, lasers that deliver high energy levels over short pulse durations, generate MTZ with less coagulation compared to low-power devices.

AFL technique is primarily used in dermatology for skin rejuvenation and remodeling of scar tissue. However, in 2010 the use of AFL to facilitate uptake of topically applied drugs was introduced [11–13]. In intact skin, the outermost layer, *stratum corneum*, constitutes an important barrier for uptake of topically applied drugs [14,15]. Corneocytes densely embedded in a hydrophobic non-polar lipid matrix make the skin practically impermeable for hydrophilic and charged molecules, and a molecular weight (MW) of 500 Da is the approximate upper limit for passive diffusion of lipophilic drugs [15–17]. AFL exposure disrupts the skin barrier and the generated MTZ comprise an alternative route for transcutaneous drug uptake and biodistribution. At present, several studies have demonstrated that AFL exposure intensifies skin uptake of topically applied drugs and enhances transcutaneous delivery [10,12,18–27]. Furthermore, studies have shown that AFL exposure enables topical administration of molecules with MWs up to 150 kDa [28–34]. AFL-assisted drug delivery has been applied for treatment of various clinical conditions, primarily for precancerous lesions and non-melanoma skin cancer [35–41] but also for hypertrophic scars [42] and skin rejuvenation [43]. Potential use of the technique in topical anesthetic and vaccinations has also been explored [25,34].

Earlier experimental studies have focused on the impact of specific laser settings in terms of AFL channel density and depth for AFL-assisted drug delivery [10,11,13,23,44]. However, knowledge on the importance of CZ for uptake and distribution of topically applied compounds is limited and has so far only been partly addressed in two former studies [31,44]. In this study, under standardized conditions we compared the uptake of topically applied compounds through micro-channels surrounded by none (0 μm), thin (20 μm), and thick (80 μm) CZ. The influence of the CZ was investigated for molecules with MWs ranging from 350 to 5,000 Da. Unexpected insight was found into the importance of CZ for skin uptake, dermal, and transdermal distribution of topically applied hydrophilic compounds.

METHODS

Study Design

Intra- and transcutaneous delivery of topically applied test compounds through microchannels with variable CZ thickness was investigated in a Franz Cell model. Interventions ($n = 16$) comprised microchannels surrounded by a CZ thickness of 0, 20, and 80 μm (CZ-0, CZ-20, and CZ-80) generated by microneedles (MN) and AFL (10,600 nm) exposure (Table 1). Penetration depth as well as number of applied microchannels per skin area was standardized between interventions. Selected test compounds were fluorescent labeled polyethylene glycols (PEGs) with mean MW of 350, 1,000, and 5,000 Da. Intra- and transcutaneous delivery was evaluated after an incubation time of 4 hours. Intracutaneous uptake in CZ and dermis was analyzed in selected regions of interest (ROI) by fluorescence microcopy, and transcutaneous permeation quantified by fluorescence intensity measures of receptor fluids. A total of 144 skin samples were included comprising nine repetitions of each intervention (Table 1).

Skin Preparation and Formation of Microchannels

Full-thickness porcine skin was collected from the flank of a 40 kg female Danish landrace/Yorkshire pig immediately after euthanasia. All skin samples originated from the flank region to minimize variations in skin structure and thickness. Hair was trimmed, subcutaneous fat removed and skin was cut in square patches of approximately 2×2 cm before storage at -80°C for up to 2 months, before randomly assigned to interventions. Thus, all samples were subjected to similar freezing procedure prior to experiment, and the time to AFL/MN procedures after samples were taken out of the freezer was the only procedural variation between interventions. CZ-0 microchannels were generated by a 1.0 mm MN dermaroller (DRS® DermaRoller) applied to frozen skin (–20°C). Under a constant firm pressure, four MN passes were applied to each skin sample in a standardized pattern. The Dermaroller was rotated 45° between each of the four passes, and generated 216 microchannels per cm^2 skin. AFL channels were applied by a 10,600 nm fractional CO_2 laser system (UltraPulse®, DeepFx handpiece, Lumenis Inc., Santa Clara, CA). CZ-20 was generated by a single pulse of 50 mJ/mb (60 W, 600 Hz) applied to deep frozen skin (–80°C) and CZ-80 by single pulse 40 mJ/mb (15 W, 150 Hz) applied to skin equilibrated to room temperature (+20°C). AFL density of 5% corresponded to 196 laser channels per cm^2 skin area. Microchannel densities as well as penetration depths were matched between interventions before study initiation by pre-study experiments to establish relations between skin temperature, AFL settings and resultant CZ- and microchannel dimensions.

Final dimensions of included microchannels were histologically confirmed from light microscopy images of vertical skin sections ($n \geq 6$) from each intervention (Fig. 1).

Test Compounds

PEGs are chemically stable, charge neutral, hydrophilic polymers. Fluorescein isothiocyanate (FITC) labeled PEG's with peak excitation at 495 nm and peak emission at 520 nm are commercially available and FITC-PEGs with MW of 350, 1,000, and 5,000 Da were selected as test molecules (Catalog no. PG1-FC-350, PG1-FC-1k and PG1-FC-5k, Nanocs, Boston, MA). Passive diffusion of test compounds is driven by the concentration gradient across skin, that is, between Franz Cell donor and receptor fluids.

TABLE 1. Interventions and Data on Transcutaneous Permeation

	Impedance		Receptor permeation	Relative ratio	
Interventions	Median (IQR), kΩ	Applied to donor	Median (IQR), mol/L	Donor/receptor	*P* values
1. CZ-0 + PEG 350	4.1 (3.8–4.3)	1.43E–3 mol/L (0.50 mg/ml)	3.41E-07 (2.61E-07–4.32E-07)	4,189	<0.001 (CZ-80 vs. CZ-0)
2. CZ-20 + PEG 350	4.0 (3.9–4.1)		6.89E-07 (5.73E-07–7.84E-07)	2,075	<0.001 (CZ-20 vs. CZ-0)
3. CZ-80 + PEG 350	3.9 (3.8–3.9)		4.26E-07 (2.22E-07–5.43E-07)	3,355	<0.001 (CZ-80 vs. CZ-20)
4. NT + PEG 350	37.3 (24.0–52.3)		0	–	–
5. CZ-0 + PEG 1000	3.7 (3.6–4.1)	1.43E–3 mol/L, 1.43 mg/ml	9.84E-08 (8.32E-08–1.50E-07)	14,526	<0.001 (CZ-80 vs. CZ-0)
6. CZ-20 + PEG 1000	4.1 (3.9–4.4)		1.10E-07 (6.43E-08–1.59E-07)	13,006	ns (CZ-20 vs. CZ-0)
7. CZ-80 + PEG 1000	4.0 (3.8–4.2)		3.47E-08 (2.17E-08–4.55E-08)	41,195	=0.001 (CZ-80 vs. CZ-20)
8. NT + PEG 1000	28.8 (21.4–44.6)		0	–	–
9. CZ-0 + PEG 5000	4.1 (3.7–5.1)	1.43E–3 mol/L, 7.14 mg/ml	7.38E-08* (6.96E-08–9.37E-08)	19,386	–
10. CZ-20 + PEG 5000	3.9 (3.5–4.2)		9.97E-08* (7.31E-08–1.58E-07)	14,338	ns (CZ-20 vs. CZ-0)
11. CZ-80 + PEG 5000	3.9 (3.8–4.0)		0*	–	–
12. NT + PEG 5000	48.9 (25.3–7.6)		0	–	–
13. CZ-0 + PBS	4.1 (4.0–6.0)	0			
14. CZ-20 + PBS	4.1 (3.6–4.2)				
15. CZ-80 + PBS	4.5 (4.0–5.4)				
16. NT + PBS	30.2 (22.0–48.6)				

Each intervention included $n = 9$ repetitions.
CZ-20/CZ-80: Ablative fractional laser exposed skin with microchannels surrounded by 20 and 80 μm coagulation zone.
CZ-0: Skin exposed to micro-needles generating channels with no coagulation zone.
NT, Non-treated skin samples.
PEG, Polyethylene glycols with mean MW of 350, 1,000, and 5,000 Da.
*Transcutaneous permeation was detectable in 2, 7, and 5 of $n = 9$ receptor chambers in intervention 9, 10, and 11, respectively.

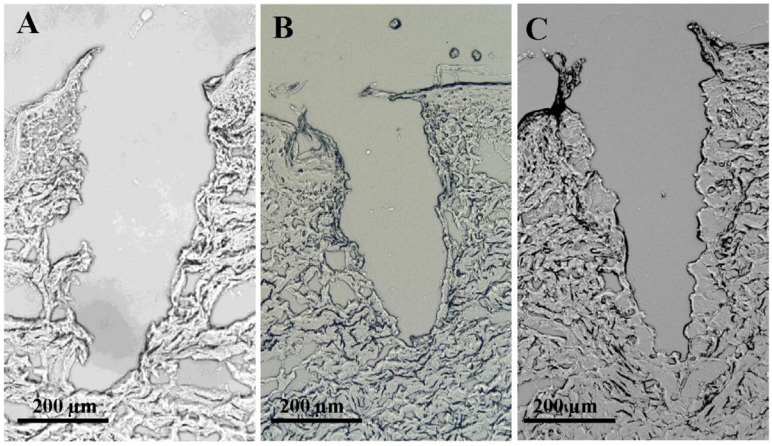

Fig. 1. Vertical sections of microchannels generated from (**A**) micro-needle (MN) exposure with 1.0 mm dermaroller (**B**) ablative fractional laser (AFL) exposure on frozen skin (50 mJ/pulse) and (**C**) AFL exposure on skin of room temperature (40 mJ/pulse).

Therefore, we prepared FITC-PEG stock solutions of similar molarities (M, mol/L). Stock solutions of 0.50, 1.43, and 7.14 mg/ml were prepared for FITC-PEG 350, 1,000, and 5,000, respectively in phosphate buffered saline (PBS), corresponding to a donor concentration of 1.43 mM.

Franz Cells

Franz Cells is a well-established and widely used model for studies in the field of cutaneous drug delivery [13,21,30,45]. Skin samples were mounted in vertical Franz Cells (PermeGear Inc., Hellertown, PA) with a permeation area of 0.64 cm^2. The 5 ml receptor chambers were filled with PBS (Ph 7.4), and 1.3 ml of either a PEG stock solution or PBS was applied to donor chambers. Circulating water of 37°C surrounded each Franz Cell and maintained skin temperature at 32°C, and magnetic stir bars swirled receptors fluids. Impedance as surrogate measure for skin barrier integrity was measured across the skin to ensure skin barriers were representative within interventions (EIM105 Prep-check Electrode Impedance Meter, General Devices, Ridgefield, NJ) [46,47]. Permeations studies ran for 4 hours, and therefore uptake of PEGs were evaluated before reaching equilibrium between donor, skin, and receptor compartments. At the end of the 4 hour permeation period, donor and receptor fluids were collected and skin demounted. An 8 mm punch biopsy was collected from each skin sample and immediately stored at −80°C. To avoid photobleaching of FITC, all experiments were conducted in a dark room when necessary dim red light was used.

Fluorescence Microscopy of Skin Sections

From frozen skin biopsies ($n = 144$) horizontal sections of 10 μm thickness were collected at three specific skin depths of 150, 400, and 1,000 μm (±10) resulting in a total of $n = 432$ sections. Digital fluorescence microscopy was performed on an IMIC microscopy system (Till-Photonics/FEI GmbH, Munich, Germany). Digital images of fluorescence were captured from the central part of each skin section. Sections were illuminated for 20 milliseconds with 488 nm monochromatic light (Monochromator: Poly V, 15 nm bandwidth, Till-photonics/FEI GmbH) by a 150 W direct current Xenon lamp with maximum light fluctuation of 1% (Hamamatsu Super Quiet, Shizuoka-ken, Japan). Stability in fluorescence intensity of excitation light was controlled at each microscopy session on a fluorescent standard slide (Chroma Technology Corp., Bellows Falls, VT). Corresponding bright field images were taken from all sections and captured by a 12-bit gray-scale CCD camera at ×10 magnification (Hamamatsu ORCA 03, Shizuokaken, Japan).

Digital images were processed and analyzed in ImageJ (version 1.49n, National Institutes of Health, MD). Background fluorescence was determined on each slide and subtracted from measured skin values. Dermal fluorescence intensities were assessed within a fixed standardized circular region of interest (ROI, diameter = 670 μm) with even microscopic light luminesce (±5%) defined from the fluorescent standard slide (Fig. 2). In calculation of mean dermal fluorescence intensities, skin areas with sebaceous glands, sweat glands, and hair follicles were excluded.

Coagulation zones in AFL interventions were manually defined on bright field microscopy images (Fig. 2) and transferred to corresponding fluorescence images. Fluorescence intensity inside the defined CZ area was expressed as both mean fluorescence intensity and the total fluorescence count of the entire CZ area.

Transcutaneous Fluorescence Intensity

Fluorescence intensities of FITC-PEG in receptor champers were quantified using a plate reader (Victor$_{TM}$, Wallac 1420Multilabel Counter, PerkinElmer Life and Analytical Sciences, Turku, Finland). From each receptor

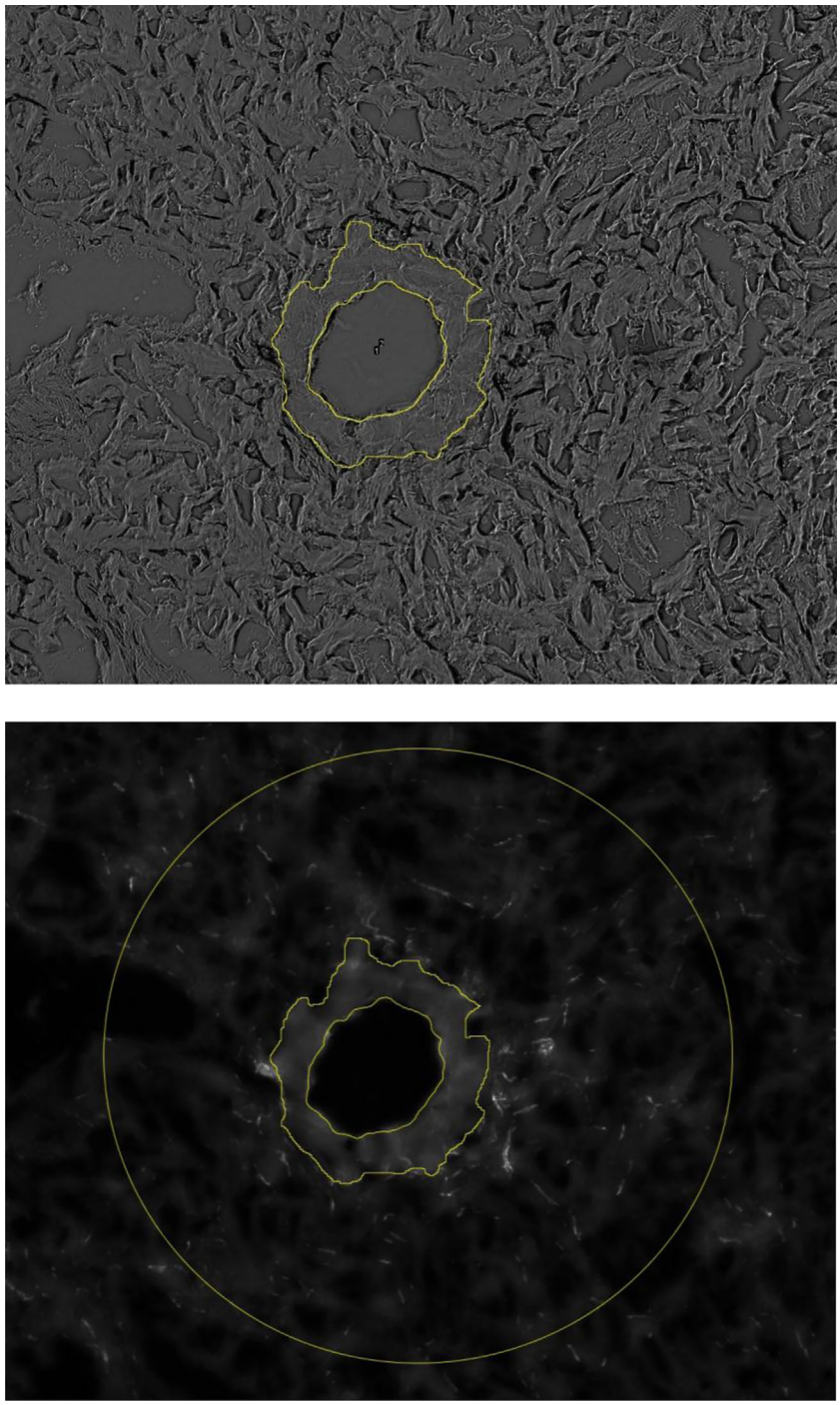

Fig. 2. Coagulation zones (CZ) in AFL interventions were manually defined on bright field microscopy images and transferred to corresponding fluorescence images. Fluorescence intensities were assesses within a standardized circular fixed region of interest (ROI) with a diameter of 670 μm, marked by a yellow circle on the lower image.

chamber, 0.4 ml samples were transferred into an 18-well plastic plate; PBS control samples were included. A tungsten-halogen continuous wave lamp with a 482 nm (470–490 nm) excitation filter illuminated samples and fluorescence counts were measured over 0.5 seconds using a 545 nm (520–560 nm) emission filter. Concentration of FITC-PEG was hereafter estimated from standard curves describing relations between fluorescence counts and FITC-PEG concentrations. The median fluorescence count from PBS control interventions +2 SD was used to define the lower detection-limit for transcutaneous FITC-PEG permeation.

Statistics

Non-parametric analyses were selected because normal distribution of data could not be assured due to small sample sizes. Mann–Whitney *t*-test was used for two-group comparisons and Kruskal–Wallis test for more than two-group comparisons. *P* values less than 0.05 were considered significant. Statistics was performed using PRISM® GraphPad, version 4.03 (GraphPad Software inc., La Jolla, CA).

RESULTS

Dimensions of Microchannels

Microchannel dimensions are visualized in Figure 1, showing A) CZ-0 from MN exposure and B) CZ-20 (median 21, range 14–25 μm) and C) CZ-80 (median 70, range 45–106 μm) from AFL exposure. All microchannels reached into mid-dermis with median penetrations depths of 600 μm (CZ-20) and 700 μm (CZ-0 and CZ-80). Widths of applied channels were median 151 μm (CZ-0), 202 μm (CZ-20), and 172 μm (CZ-80). Median surface areas within the generated microchannels were estimated by use of the formula for a cylinder (concave area of a cylinder ((Pi × width × height) × (no. of channels per cm^2 skin area)). The three microchannel profiles generated comparable surface areas (±4%) for uptake of topical compounds of 0.72 cm^2 (CZ-0), 0.75 cm^2 (CZ-20), and 0.74 cm^2 (CZ-80) per cm^2 skin area.

Skin Uptake

Representative images of PEG 1,000 fluorescence in CZ-0, CZ-20, and CZ-80 as well as in non-exposed skin samples are illustrated in Figure 3. Qualitative evaluation of fluorescence images demonstrated intensified uptake of PEGs trough CZ-0, CZ-20, and CZ-80 compared to non-exposed skin. Regarding PEG bio-distribution, fluorescence intensities were visibly higher inside CZs than in surrounding dermis in both CZ-20 and CZ-80 interventions. In CZ-0, fluorescence were more intense in dermal areas immediately adjacent to the microchannels compared to remaining dermal skin areas. In non-exposed skin samples, fluorescence intensities were generally low (Fig. 3).

Fluorescence in coagulation zones. Total fluorescence counts of PEGs inside CZ areas are illustrated in Figure 4 whereas mean fluorescence intensities of PEGs in CZs are illustrated in Figure 5. There were similar total fluorescence counts inside CZ-20 and CZ-80 areas for all PEG MW ($P > 0.0503$; PEG 350, 1,000, and 5,000) (Fig. 4). However, mean fluorescence intensities within CZs were significantly higher in CZ-20 compared to CZ-80 independent of PEG size (PEG 350, 1,000, and 5,000; $P < 0.0001$). Thus, the total accumulation of fluorescence was similar in CZ-20 and CZ-80 areas (Fig. 4), but fluorescence was deposited at significantly higher intensities in CZ-20 compared to CZ-80 (Fig. 5). Finally, looking at the distribution of fluorescence from superficial to deeper skin layers, data demonstrated similar mean fluorescence intensities at 150 and 400 μm skin depth in both CZ-20 and CZ-80 interventions (PEG 350, 1,000, and 5,000, $P > 0.162$) (Fig. 5).

Fluorescence in dermis. Distribution of PEGs into dermis through microchannels is illustrated in Figure 6. Overall, dermal fluorescence intensities were significantly affected by thickness of CZ. Thus, dermal fluorescence intensities were higher in interventions with CZ than without CZ (CZ-20 and CZ-80 > CZ-0; Fig. 6). Moreover, dermal fluorescence intensities in CZ-20 interventions were significantly higher compared to both CZ-0 and CZ-80 interventions from superficial to deep skin layers (PEG 350, 1,000, and 5,000, 150 μm to 1,000 μm; $P < 0.001$). Although dermal fluorescence intensities were higher in CZ-80 compared to CZ-0 interventions, results did not reach significance for all PEG MW. Dermal uptake through CZ-80 was superior to CZ-0 for the smallest test compound, PEG 350 (150–1,000 μm, $P < 0.001$), but for PEG 1,000 and 5,000 the advantage of CZ-80 over CZ-0 was minor and not significant at all skin layers.

Vertical biodistribution of PEGs from superficial to deeper dermal skin layers was affected by MW (Fig. 6). For PEG 350, fluorescence intensities were similar in superficial (150 μm) and deep (1,000 μm) skin layers, independent of CZ thickness (CZ-0, CZ-20, and CZ-80; $P > 0.114$). For PEG 1,000, fluorescence intensities decreased from 400 to 1,000 μm skin depth in CZ-20 ($P = 0.004$) but not in CZ-0 and CZ-80 interventions ($P < 0.05$). Finally, for the largest test compound, PEG 5,000, fluorescence intensities were significantly lower in deep (1,000 μm) compared to superficial (140μm) dermis, independent of CZ thickness (CZ-0, CZ-20, and CZ-80; $P < 0.040$). In PEG interventions with unexposed skin samples, dermal fluorescence intensities were similar to PBS control interventions. Thus PEG uptake in unexposed skin was below detection limit.

Transcutaneous Permeation

Results on transcutaneous permeation of PEGs are given in Table 1. In general, CZ-20 facilitated the highest skin permeation, but the impact of the CZ thickness was affected by PEG molecular weight. For PEG 350, transcutaneous permeation through CZ-20 was significantly higher than through CZ-0 and CZ-80 ($P < 0.001$), but for PEG 1,000 permeation through CZ-20 was only significantly higher than CZ-80, whereas the difference to CZ-0 was insignificant. For PEG 5,000, transcutaneous permeation was generally low and only above the detection limit in five of nine samples (CZ-0), seven of nine (CZ-20), and two of nine (CZ-80).

MW of PEGs substantially affected the intensity of transdermal permeation, with lower permeation of larger compared to smaller molecules. In CZ-20 interventions, the relative concentration of PEG in donor versus receptor chamber (donor molarity/ receptor molarity) increased from 2,075 (PEG 350) to 13,006 (PEG 10,000) and 14,338 (PEG 5,000) (Table 1). Thus, transcutaneous permeation was reduced sevenfold (14,338/2,075) by enlarging MW from 350 to 5,000 Da. In CZ-0 and CZ-80 interventions, transcutaneous permeation also decreased at larger MWs, but permeation of PEG 5,000 was generally low, therefore donor/receptor relations were uncertain. In non-exposed

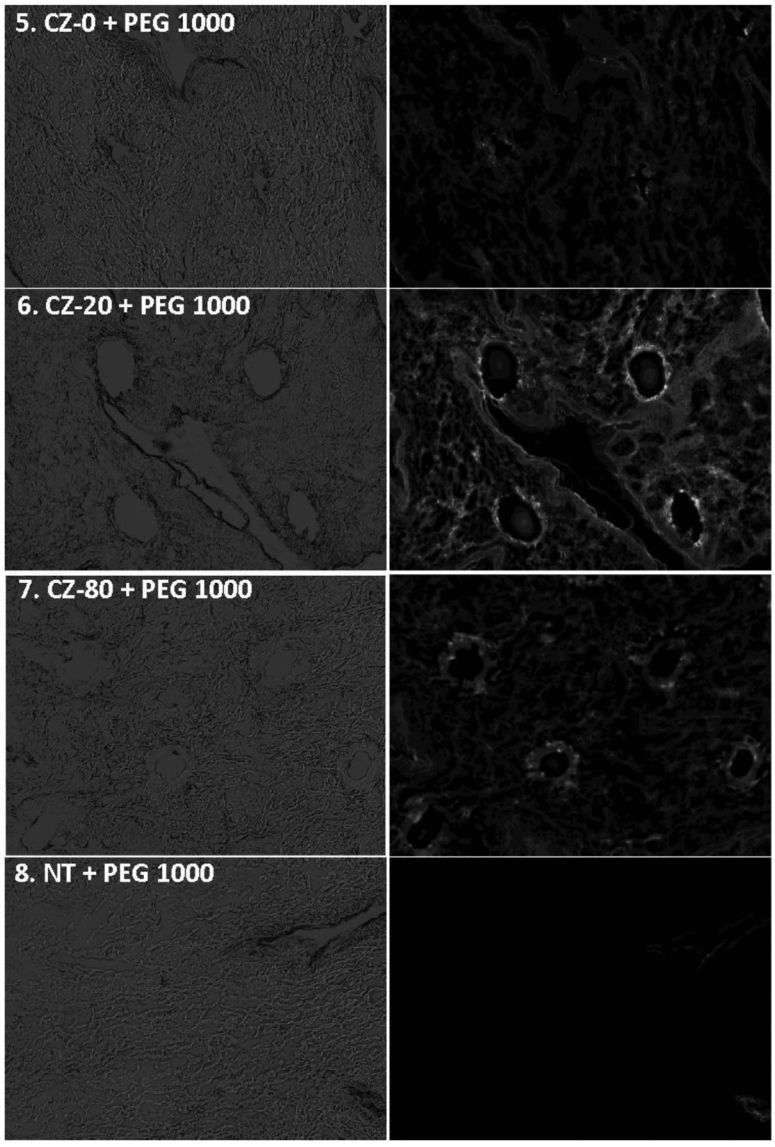

Fig. 3. Horizontal sections at a 150 μm skin depth illustrating wide-field and corresponding fluorescence images. Intensified fluorescence was observed from CZ-0, CZ-20, and CZ-80 interventions compared to non-treated (NT) skin.

skin samples, we detected no transcutaneous permeation of PEGs.

DISCUSSION

Limited information is available on the impact of AFL generated CZ for uptake of topically applied drugs. This study presents novel insight on the influence of variable clinically relevant CZ thicknesses for permeation and distribution of topically applied test compounds, which may be important for controlled AFL-assisted drug delivery. Surprisingly, the presence of a thin coagulation zone increased uptake of topical compounds.

Overall, the AFL-induced CZ enhanced skin uptake of PEGs since fluorescence intensities were higher in CZ-20 and CZ-80 interventions compared to CZ-0 interventions. The total accumulation of PEGs in CZ areas was similar in a thin 20 μm and thick 80 μm CZ, but CZ thickness had significant effect on intracutaneous distribution of PEGs. Thus, both inside CZ as well as in surrounding dermal skin PEGs accumulated in higher concentrations from CZ-20 compared to CZ-80 interventions. The data indicate that a small amount of thermal coagulation is an advantage for hydrophilic topical drug uptake, and that the thickness of CZ may potentially be used to control intracutaneous drug distribution.

To our knowledge, two former studies have evaluated the importance of variable CZ thickness for uptake of topically applied compounds. Lee et al. compared drug uptake from fractional CO_2 versus Er:YAG exposure [31]. In vitro data from this study suggested comparable

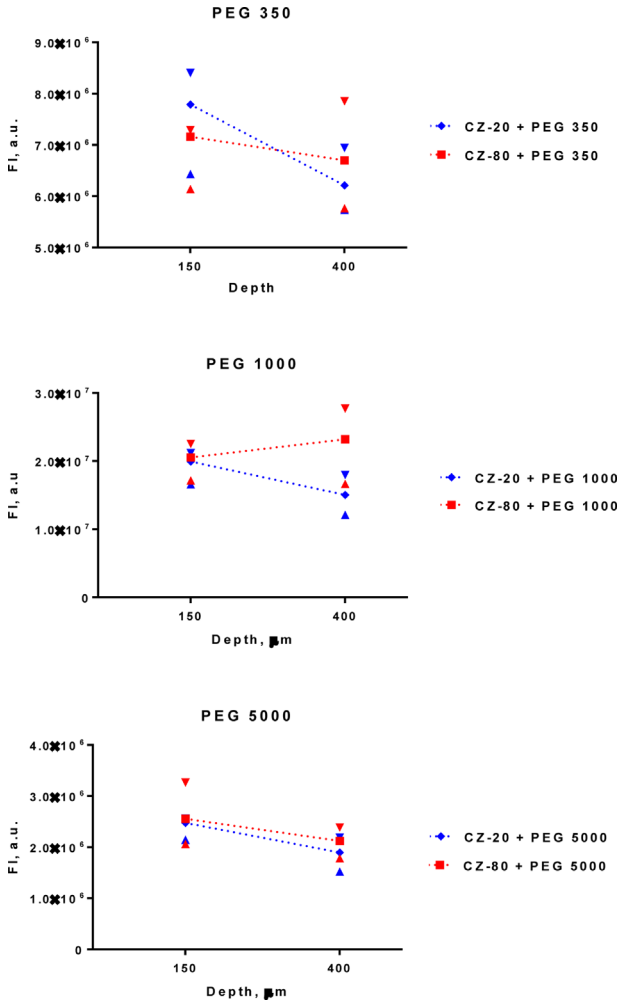

Fig. 4. Illustrate total fluorescence counts in CZ areas at 150 and 400 µm skin depths. Total fluorescence accumulation inside CZ-20 and CZ-80 was similar for all PEG molecular weights. Medians are illustrated with IQR ranges.

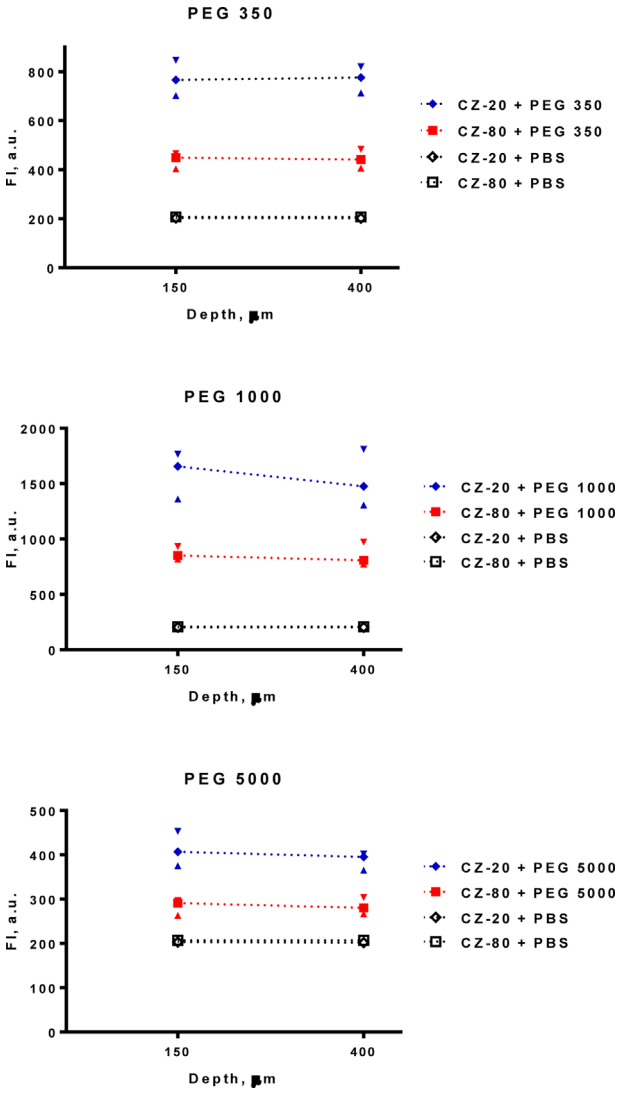

Fig. 5. Illustrates mean fluorescence intensities in CZ areas from PEG 350, 1,000, and 5,000 application. Mean fluorescence intensities in CZ areas were significantly higher in the thin CZ-20 compared to the thick CZ-80 from both PEG 350, 1,000, and 5,000 application. Medians are illustrated with IQR ranges.

transcutaneous drug permeation, but *in vivo* data found more-efficient intracutaneous distribution from fractional CO_2 compared to Er:YAG exposure. Taudorf et al. evaluated uptake of topically applied MTX from Er:YAG laser exposure, applying three different laser settings and generating microchannels with CZ thicknesses ranging from 6 to 47 µm [44]. Uptake was evaluated after 21 hours incubation and similar concentrations of MTX was found in CZ and surrounding dermis. The primary focus of the above mentioned studies was not to investigate the importance of CZ and it is unknown how CZ thickness affected the results. Thus, differences in the generated surface areas for drug uptake may have affected these results. Moreover, with a 21 hours long incubation time Taudorf et al. investigated distribution of MTX after the skin was saturated. In contrast, we evaluated intracutaneous distribution of PEGs at 4 hours incubation before skin samples reached saturation.

Our study directly compared uptake of test compounds through microchannels with variable CZ thickness. The mid-dermal penetration depths of microchannels, and number of channels per skin area were held constant, while CZ thickness was varied from 0 to 80 µm. We found that in this study topical compounds penetrate and partition easier within a 20 µm thin than an 80 µm thick CZ. This is presumably due to CZ thickness, but other explanations are possible. We used frozen tissue ablation to create the 20 µm CZ samples, whereas the 80 µm CZ samples were ablated at room temperature. We examined the possibility that CZ structure or surrounding dermal skin areas were different between these samples by light microscopy, which showed no apparent differences in density or structure. Another explanation could be differences in water content within a thick and thin CZ. Future

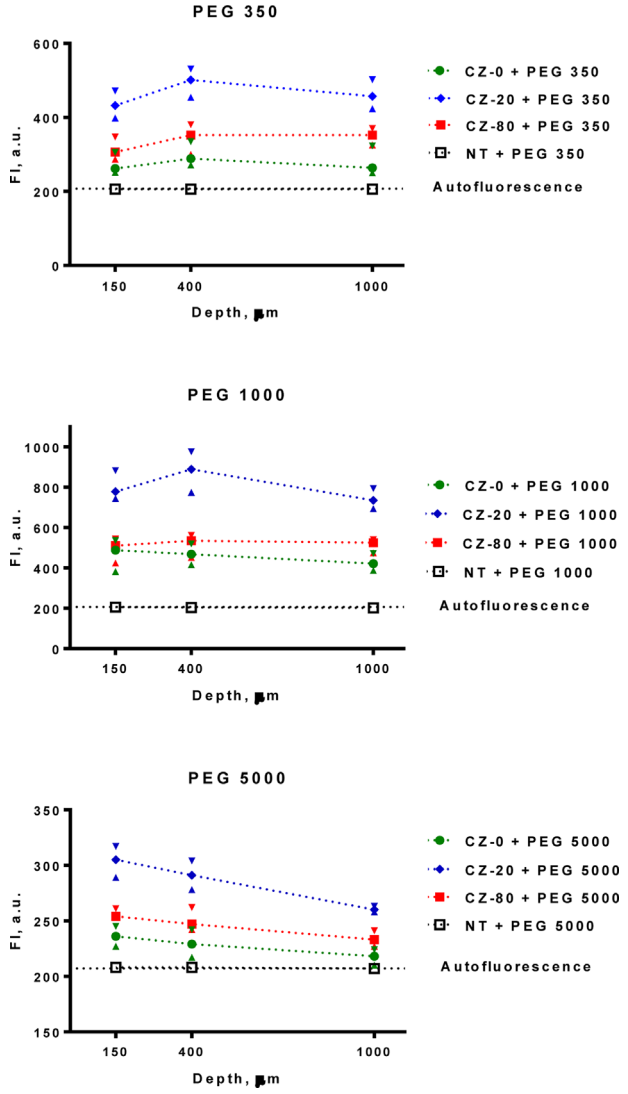

Fig. 6. Mean dermal fluorescence intensities illustrate higher PEG uptake through CZ-20 compared to CZ-80 and CZ-0 for both PEG 350, 1,000, and 5,000. For PEG 350 uptake through CZ-80 was significantly higher than through CZ-0 throughout skin depths. For PEG 1,000 and 5,000 differences in uptake through CZ-80 and CZ-0 were less pronounced and only reach significance at some skin depths (PEG 1,000: $P = 0.002$ at 1,000 μm depth; PEG 5000: $P < 0.004$ at 400 and 1,000 μm).

evaluations of specific skin structures by electron microscopy may add additional information to laser–tissue interactions at different skin temperatures.

Test compounds of 350, 1,000, and 5,000 Da were selected to mimic penetration across an AFL processed skin barrier for drugs of different MW. Intensified uptake through microchannels was documented for the MW range of drugs included. In line with our results on PEG 350, a former study on topical uptake of MTX (453 Da) found that the CZ imposed little or no barrier for drug uptake, and that MTX is rapidly distributed inside CZ [29]. In contrast, for larger molecules (PEG 1,000 and 5,000) we found that the dermal distribution through CZ-80 was only slightly higher than trough CZ-0 and not significant at all skin depths, whereas uptake through CZ-20 was significantly higher compared to CZ-0. Uptake of these compounds at the same donor concentration is affected mainly by two factors, the partition coefficient between donor solution and skin, and the diffusion constant within the tissue. Without more detailed kinetic data within each compartment (CZ, dermis, transdermal receptor), it is impossible to conclude at this time which factors are primarily responsible for the observed effect of CZ thickness on permeation of the compounds tested.

A major limitation of this study is that it is based on an *in vitro* model that eliminates the potential effects of tissue fluid oozing and bleeding after AFL treatment. Moreover, in our study there was no systemic uptake of applied compounds into the bloodstream. Another important limitation is that the study was conducted on skin that had been frozen, which may alter the mechanical properties of skin and hereby transdermal drug diffusion [48,49]. The results provide motivation and guidance for future *in vivo* studies.

In conclusion, this standardized controlled study is the first to examine the role of CZ on uptake and skin permeation of topical hydrophilic compounds at various molecular weights. We found higher uptake through microchannels surrounded by a CZ than with no CZ. Moreover, thickness of the CZ was important for skin distribution and compounds accumulated at higher concentrations through MTZs with 20 μm compared to 80 μm CZ. These findings suggest that AFL-assisted delivery of topical compounds can be controlled by choice of CZ thickness, among other parameters. The precision of AFLs to control density, depth, diameter, and CZ thickness for greatly enhanced delivery of drugs into skin, is promising.

REFERENCES

1. Manstein D, Herron GS, Sink RK, Tanner H, Anderson RR. Fractional photothermolysis: A new concept for cutaneous remodeling using microscopic patterns of thermal injury. Lasers Surg Med 2004;34(5):426–438.
2. Hantash BM, Bedi VP, Chan KF, Zachary CB. Ex vivo histological characterization of a novel ablative fractional resurfacing device. Lasers Surg Med 2007;39(2):87–95.
3. Hantash BM, Bedi VP, Kapadia B, et al. In vivo histological evaluation of a novel ablative fractional resurfacing device. Lasers Surg Med 2007;39(2):96–107.
4. Bogdan Allemann I, Kaufman J. Fractional photothermolysis—An update. Lasers Med Sci 2010;25(1):137–144.
5. Tannous Z. Fractional resurfacing. Clin Dermatol 2007;25(5):480–486.
6. Anderson RR, Parrish JA. Selective photothermolysis: Precise microsurgery by selective absorption of pulsed radiation. Science 1983;220(4596):524–527.
7. Paasch U, Haedersdal M. Laser systems for ablative fractional resurfacing. Expert Rev Med Devices 2011;8(1):67–83.
8. Shin MK, Choi JH, Ahn SB, Lee MH. Histologic comparison of microscopic treatment zones induced by fractional lasers and radiofrequency. J Cosmet Laser Ther 2014;16(6):317–323.
9. Farkas JP, Richardson JA, Burrus CF, Hoopman JE, Brown SA, Kenkel JM. In vivo histopathologic comparison of the acute injury following treatment with five fractional ablative laser devices. Aesthet Surg J 2010;30(3):457–464.
10. Haak CS, Farinelli WA, Tam J, Doukas AG, Anderson RR, Haedersdal M. Fractional laser-assisted delivery of methyl

aminolevulinate: Impact of laser channel depth and incubation time. Lasers Surg Med 2012;44(10):787–795.
11. Forster B, Klein A, Szeimies RM, Maisch T. Penetration enhancement of two topical 5-aminolaevulinic acid formulations for photodynamic therapy by erbium:YAG laser ablation of the stratum corneum: Continuous versus fractional ablation. Exp Dermatol 2010;19(9):806–812.
12. Hædersdal M, Sakamoto FH, Farinelli WA, Doukas AG, Tam J, Anderson RR. Fractional CO2 laser-assisted drug delivery. Lasers Surg Med 2010;42(2):113–122.
13. Lee WR, Shen SC, Pai MH, Yang HH, Yuan CY, Fang JY. Fractional laser as a tool to enhance the skin permeation of 5-aminolevulinic acid with minimal skin disruption: A comparison with conventional erbium:YAG laser. J Control Release 2010;145(2):124–133.
14. Madison KC. Barrier function of the skin: "La Raison d'Être" of the epidermis. J Investig Dermatol 2003;121(2):231–241.
15. Brown MB, Martin GP, Jones SA, Akomeah FK. Dermal and transdermal drug delivery systems: Current and future prospects. Drug Deliv 2006;13(3):175–187.
16. Benson HA. Transdermal drug delivery: Penetration enhancement techniques. Curr Drug Deliv 2005;2(1):23–33.
17. Bos JD, Meinardi MM. The 500 Dalton rule for the skin penetration of chemical compounds and drugs. Exp Dermatol 2000;9(3):165–169.
18. Lin CH, Aljuffali IA, Fang JY. Lasers as an approach for promoting drug delivery via skin. Expert Opin Drug Deliv 2014;11(4):599–614.
19. Bloom BS, Brauer JA, Geronemus RG. Ablative fractional resurfacing in topical drug delivery: An update and outlook. Dermatol Surg 2013;39(6):839–848.
20. Marra DE, Yip D, Fincher EF, Moy RL. Systemic toxicity from topically applied lidocaine in conjunction with fractional photothermolysis. Arch Dermatol 2006;142(8):1024–1026.
21. Yu J, Bachhav YG, Summer S, et al. Using controlled laser-microporation to increase transdermal delivery of prednisone. J Control Release 2010;148(1):e71–e73.
22. Haedersdal M, Sakamoto FH, Farinelli WA, Doukas AG, Tam J, Anderson RR. Pretreatment with ablative fractional laser changes kinetics and biodistribution of topical 5-aminolevulinic acid (ALA) and methyl aminolevulinate (MAL). Laser Surg Med 2014;46(6):462–469.
23. Haak CS, Bhayana B, Farinelli WA, Anderson RR, Haedersdal M. The impact of treatment density and molecular weight for fractional laser-assisted drug delivery. J Control Release 2012;163(3):335–341.
24. Oni G, Brown SA, Kenkel JM. Can fractional lasers enhance transdermal absorption of topical lidocaine in an in vivo animal model? Lasers Surg Med 2012;44(2):168–174.
25. Meesters AA, Bakker MM, De Rie MA, Wolkerstorfer A. Fractional CO laser assisted delivery of topical anesthetics: A randomized controlled pilot study. Lasers Surg Med 2016;48(2):208–211.
26. Raphael AP, Wright OR, Benson HA, Prow TW. Recent advances in physical delivery enhancement of topical drugs. Curr Pharm Des 2015;21(20):2830–2847.
27. Haedersdal M, Erlendsson AM, Paasch U, Anderson RR. Translational medicine in the field of ablative fractional laser (AFXL)-assisted drug delivery: A critical review from basics to current clinical status. J Am Acad Dermatol 2016;74(5):981–1004.
28. Erlendsson AM, Taudorf EH, Eriksson AH, et al. Ablative fractional laser alters biodistribution of ingenol mebutate in the skin. Arch Dermatol Res 2015;307(6):515–522.
29. Taudorf EH, Lerche CM, Vissing AC, et al. Topically applied methotrexate is rapidly delivered into skin by fractional laser ablation. Expert Opin Drug Deliv 2015;12(7):1059–1069.
30. Lee WR, Shen SC, Al-Suwayeh SA, Yang HH, Yuan CY, Fang JY. Laser-assisted topical drug delivery by using a low-fluence fractional laser: Imiquimod and macromolecules. J Control Release 2011;153(3):240–248.
31. Lee WR, Shen SC, Chen WY, Aljuffali IA, Suen SY, Fang JY. Noninvasive delivery of siRNA and plasmid DNA into skin by fractional ablation: Erbium:YAG laser versus CO(2) laser. Eur J Pharm Biopharm 2014;86(3):315–323.
32. Zech NH, Murtinger M, Uher P. Pregnancy after ovarian superovulation by transdermal delivery of follicle-stimulating hormone. Fertil Steril 2011;95(8):2784–2785.
33. Yu J, Kalaria DR, Kalia YN. Erbium:YAG fractional laser ablation for the percutaneous delivery of intact functional therapeutic antibodies. J Control Release 2011;156(1):53–59.
34. Chen X, Shah D, Kositratna G, Manstein D, Anderson RR, Wu MX. Facilitation of transcutaneous drug delivery and vaccine immunization by a safe laser technology. J Control Release 2012;159(1):43–51.
35. Ko DY, Kim KH, Song KH. A randomized trial comparing methyl aminolaevulinate photodynamic therapy with and without Er:YAG ablative fractional laser treatment in Asian patients with lower extremity Bowen disease: Results from a 12-month follow-up. Br J Dermatol 2014;170(1):165–172.
36. Haak CS, Togsverd-Bo K, Thaysen-Petersen D, et al. Fractional laser-mediated photodynamic therapy of high-risk basal cell carcinomas—A randomized clinical trial. Br J Dermatol 2015;172(1):215–222.
37. Togsverd-Bo K, Haak CS, Thaysen-Petersen D, Wulf HC, Anderson RR, Haedersdal M. Intensified photodynamic therapy of actinic keratoses with fractional CO(2) laser—A randomized clinical trial. Br J Dermatol 2012;166(6):1262–1269.
38. Helsing P, Togsverd-Bo K, Veierød MB, Mørk G, Hædersdal M. Intensified fractional CO2 laser-assisted photodynamic therapy vs. laser alone for organ transplant recipients with multiple actinic keratoses and wart-like lesions: A randomized half-side comparative trial on dorsal hands. Br J Dermatol 2013;169(5):1087–1092.
39. Ko DY, Jeon SY, Kim KH, Song KH. Fractional erbium: YAG laser-assisted photodynamic therapy for facial actinic keratoses: A randomized, comparative, prospective study. J Eur Acad Dermatol Venereol 2013;28(11):1529–1539.
40. Choi SH, Kim KH, Song KH. Efficacy of ablative fractional laser-assisted photodynamic therapy for the treatment of actinic cheilitis: 12-month follow-up results of a prospective, randomised, comparative trial. Br J Dermatol 2015;173(1):184–191.
41. Choi SH, Kim KH, Song KH. Efficacy of ablative fractional laser-assisted photodynamic therapy with short-incubation time for the treatment of facial and scalp actinic keratosis: 12-month follow-up results of a randomized, prospective, comparative trial. J Eur Acad Dermatol Venereol 2015;29(8):1598–1605.
42. Waibel JS, Wulkan AJ, Shumaker PR. Treatment of hypertrophic scars using laser and laser assisted corticosteroid delivery. Lasers Surg Med 2013;45(3):135–140.
43. Trelles MA, Leclère FM, Martínez-Carpio PA. Fractional carbon dioxide laser and acoustic-pressure ultrasound for transepidermal delivery of cosmeceuticals: A novel method of facial rejuvenation. Aesth Plast Surg 2013;37(5):965–972.
44. Taudorf EH, Lerche CM, Erlendsson AM, et al. Fractional laser-assisted drug delivery: Laser channel depth influences biodistribution and skin deposition of methotrexate. Lasers Surg Med 2016;48(5):519–529.
45. Rodrigues F, Alves AC, Nunes C, et al. Permeation of topically applied caffeine from a food by-product in cosmetic formulations: Is nanoscale in vitro approach an option? Int J Pharm 2016;513(1–2):496–503.
46. Davies DJ, Ward RJ, Heylings JR. Multi-species assessment of electrical resistance as a skin integrity marker for in vitro percutaneous absorption studies. Toxicol In Vitro 2004;18(3):351–358.
47. White EA, Orazem ME, Bunge AL. A critical analysis of single-frequency LCR databridge impedance measurements of human skin. Toxicol In Vitro 2011;25(4):774–784.
48. Ranamukhaarachchi SA, Lehnert S, Ranamukhaarachchi SL, et al. A micromechanical comparison of human and porcine skin before and after preservation by freezing for medical device development. Sci Rep 2016;6:32074.
49. Mansoor I, Lai J, Ranamukhaarachchi S, et al. A microneedle-based method for the characterization of diffusion in skin tissue using doxorubicin as a model drug. Biomed Microdevices 2015;17(3):9967.